Transport Properties of Trogamid: Comparison of Different Experimental Techniques*

A. Etxeberria, A. Garcia, M. Iriarte, J. J. Iruin, C. Uriarte

Departamento de Ciencia y Tecnologia de Polimeros and Instituto de Materiales Polimericos, Universidad del Pais Vasco, P.O. Box 1072, 20080 San Sebastian, Spain

Received 18 August 2005; accepted 3 January 2006
DOI 10.1002/app.24055
Published online in Wiley InterScience (www.interscience.wiley.com).

ABSTRACT: The transport properties of an amorphous polyamide, poly(trymethylhexamethylene terephtalamide) or Trogamid-T, were determined by different experimental methods. Sorption methods included two electrobalances, one for subatmospheric pressures and the other one up to 20 bar, and a pressure decay cell. Also, a permeability cell was used to measure permeability coefficients for pure gases and a gas mixture. The solubility, diffusion, and permeability coefficients calculated by different methods were in good agreement. With regard to permeability, measurements showed the difference between ideal and real permselectivity. Moreover, the results confirmed the good barrier properties of Trogamid-T. © 2006 Wiley Periodicals, Inc. J Appl Polym Sci 102: 2034–2042, 2006

Key words: barrier; diffusion; gas permeation; polyamides

INTRODUCTION

Most experimental techniques for studying the sorption, diffusion, and permeability of gases and vapors in polymers involve one of three modes of transport:[1] (1) sorption into or out of a polymer, (2) permeation through a membrane into a closed chamber, and (3) permeation through a membrane into a flowing stream.

In general, solubility coefficients (S), diffusion coefficients (D), or permeability coefficients (P) can be obtained from either sorption or permeation rate data. Sometimes, one technique is preferred over another, but any of the previously mentioned methods can be used to measure the transport properties of the material. If at all possible, however, both sorption and permeation techniques should be used to establish a comparison between the different data, and inconsistencies between results can reveal the occurrence of anomalous transport phenomena.

The sorption–desorption measurements of a penetrant in a polymer are based on the amount of penetrant that the polymer can sorb.[2] This kind of measurements provides S directly from the amount of gas absorbed once the steady state has been reached, and the rate of this process gives a direct measure of D. In these experiments, we could not directly obtain P, but it could be estimated from S and D values. In fact, if Henry's law is obeyed and the equilibrium is reached, P is given by:

$$P = DS \tag{1}$$

Most sorption measurements are performed with either a gravimetric or a barometric technique. Gravimetric methods, in which one determines sorption or desorption rate directly by following the weight change of a polymer sample. In this study, we used, among others, two gravimetric techniques. The first one used a Cahn electrobalance that provided sorption data for penetrant pressures up to 1 bar. The other one used a Hiden intelligent gravimetric analyzer (IGA) electrobalance; although it was based on the same mechanism as Cahn Balance, its design allowed us to measure gas and vapor sorption for pressures up to 20 bar. Furthermore, a complete isotherm could be performed in a unique measurement.

Moreover, when measurements are carried out at high pressures of penetrant, the sorption kinetics can be followed by the measurement of the pressure decay when the penetrant is introduced into a chamber where the polymer is placed, as described by Koros and coworkers.[3,4]

In the case of permeation methods, the measurements are based on the determination of the permeation rate of a penetrant through a polymeric membrane.

*This article is dedicated to Cecilia Sarasola.

Correspondence to: A. Etxeberria (agustin.etxeberria@ehu.es).

Contract grant sponsor: Universidad del Pais Vasco/Euskal Herriko Unibertsitatea (UPV/EHU); contract grant number: 9/UPV 00203.215-13519/2001.

Contract grant sponsor: Ministerio de Ciencia y Tecnologia (MCYT); contract grant number: MAT2002-03384.

Contract grant sponsor: Universidad del Pais Vasco/Euskal Herriko Unibertsitatea (Ph.D. grant for A.G.).

The different available devices differ in the way the permeated amount is determined. In this sense, the Lyssy apparatus is simply a permeability cell where the permeated gas or gas mixture passes to a gas chromatograph to quantify the amount of each component in the permeated mixture. The principal advantage of this technique is that it allows one to determine simultaneously the permeability of each gas when a gas mixture is used; thus, the real permselectivity is obtained.

The purpose of this study was to measure the gas-transport properties of an amorphous aromatic polyamide, poly(trymethylhexamethylene terephtalamide) named Trogamid-T (Trogamid). In general, polyamides exhibit a high cohesive energy density, an ability for very efficient chain packing, and a semicrystalline morphology. For these reasons, they normally exhibit a low gas permeability to small molecules.[5,6] In our case, the polyamide was amorphous due to the bulky noncollinear groups in the backbone that prevented chain packaging. On the other hand, aromatic polyamides, in general, have excellent thermal and mechanical properties, even better than polysulfones, which are used extensively as gas separation membranes.[7,8] With all these good properties in mind and with the knowledge that there are not yet gas-transport data of this polyamide, it could be interesting to study the gas-transport properties of Trogamid-T.

Furthermore, there is another reasons to study the Trogamid behavior as barrier material. Among the materials used as high barriers to gases and hydrocarbons, ethylene–vinyl alcohol (EVOH) random copolymers are a family of semicrystalline materials with excellent barrier properties and outstanding chemical resistance. Unfortunately, EVOH copolymers are markedly affected by water and possess a number of processing-associated problems.[9] Because of that, blends of EVOH with low contents of amorphous polyamide are claimed by manufacturers to broaden the forming capacity of EVOH with respect to temperature and draw ratios without sacrificing the gas-barrier properties at high relative humidity conditions.[10,11]

On the other hand, it is known that in some cases, such as with beer, poly(ethylene terephthalate) bottles have problems preserving the beverage properties.[12] In this sense, multilayer materials could be an alternative for obtaining the appropriate barrier properties. In such materials, both semicrystalline and amorphous polyamides are included.[13,14] Therefore, there are more reasons to study Trogamid behavior as a barrier material.

Thus, there were two complementary purposes for this study: first, the characterization of transport properties of a polymer capable of being used as barrier material and, second, a comparison of the data obtained from different techniques that would enable us to establish their reliability.

EXPERIMENTAL

Materials

Poly(2,2,4-trimethyl hexamethylene terephthalamide) or Trogamid-T-5000 was supplied by Dynamit Nobel (Kungälv, Sweden). It is an amorphous polyamide whose chemical structure is shown in the following structure:

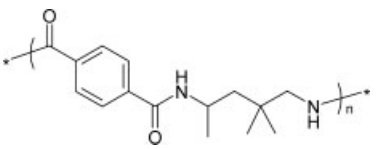

Polyamides absorb water at a rate that depends on the temperature and relative humidity. Trogamid absorbs a smaller quantity than other nylons; however, to assure the elimination of water traces, all the films were dried *in vacuo* at room temperature for at least 3 weeks. After this treatment, gravimetric measurements showed the total elimination of residual water.

Films of about 100 μg were obtained from ribbons extruded with a single-screw Brabender (Duisburg, Germany) extruder driven by a Brabender PLE 650 plasticorder. The screw had a diameter of 19 mm, a length/diameter ratio of 25, and compression ratio of 2/1. The extruder was equipped with a flat fishtail die with a cross-section of 250 mm × 0.5 mm. The extruder temperature was 230°C, and that of the die was 235°C. The ribbons were drawn with a three-roll Axon (Astorp, Sweden) drawing unit, and cooled by means of an air stream. The thickness of the membranes varied from 69 to 110 μm, as measured with a Duo-Check (Neurtek Instruments, Eibar, Spain) ST-10 apparatus. The film density was determined in a density gradient column at a value of 1.1308 g/cm^3.

Apparatus

Cahn electrobalance

A Cahn D-200 electrobalance was enclosed in a chamber thermostatized at 30°C. Before each measurement, the films were degassed in the electrobalance under a 10^{-2} mbar vacuum until a constant weight was achieved. Then, the gas was introduced at the desired pressure, up to 1 bar, and the weight gain was recorded until equilibrium was reached.

The sorption was calculated from the weight gain or total absorbed mass at equilibrium (M_∞) of the membrane after the buoyancy was corrected and a blank run was subtracted by means of the following equation:

$$C\left(\frac{\text{cm}^3\text{STP}}{\text{cm}^3}\right) = \frac{22,414 M_\infty}{44 V_{plm}} \tag{2}$$

where V_{plm} is the volume occupied by the sample (cm^3), M_∞ is the total absorbed mass at equilibrium (g),

and 44 is the molecular weight of the penetrant, in our case CO_2. Then, S, used later to obtain P, was given by this simple equation:

$$S = \frac{C}{p} \tag{3}$$

where p is the pressure. Moreover, D's were available after an appropriate mathematical treatment of the kinetic data. In this sense, the solution of Fick's second law depends on the geometry and concentration conditions. For thin-film geometry, in which diffusion from the edges of the film can be neglected and which is suddenly in an atmosphere with a constant penetrant pressure and with a constant D is assumed, the total mass uptake of the penetrant can be described by[15]

$$\frac{M_t}{M_\infty} = 1 - \frac{8}{\pi^2}\sum_{n=0}^{\infty}\frac{1}{(2n+1)^2}\exp\left(-\frac{D(2n+1)^2\pi^2 t}{l^2}\right) \tag{4}$$

where M_t is the absorbed gas at time t, l is the film thickness, and D is the diffusion coefficient (cm^2/s). If the so-called long times (50–90% of M_∞) approximation is taken into account, eq. (4) can be written as

$$\frac{M_t}{M_\infty} = 1 - \frac{8}{\pi^2}\exp\left(-\frac{D\pi^2 t}{l^2}\right) \tag{5}$$

and D can be calculated from an adequate plot of the sorption kinetic data.

Hiden IGA electrobalance

The Hiden IGA design integrates precise computer control and measurement of weight change, pressure, and temperature to enable the fully automated and reproducible determination of gas and vapor adsorption–desorption isotherms and isobars in diverse operating conditions.

The reactor was thermostated at 25°C by a water bath. The films were degassed in the electrobalance under a vacuum of 10^{-7} torr until a constant weight was achieved. Then, the gas was introduced for 2 min until the desired pressure was achieved, and the weight gain was recorded until equilibrium was reached. Later, the pressure was increased in the same way to the next pressure, and a new sorption kinetic was carried out. This step was repeated until the isotherm was completed. With the asymptotic form of sorption kinetics taken into account and to reduce the required experimental time, the software of the equipment allowed us to fit the kinetic sorption to estimate M_∞ and also allowed us to stop the sorption kinetic without having achieved the M_∞ value. In this study, a M_∞ of 99% was used to stop the kinetics. However, the software used a M_∞ of 100% in further computations and also corrected the buoyancy effect in M_∞.

Moreover, the IGA software fit Fickian kinetics by the following equation:

$$\frac{M_t}{M_\infty} = 1 - \exp\left(-\frac{t}{k}\right) \tag{6}$$

where k is a time exponential constant (s). Comparing eqs. (5) and (6), it can be deduced that the parameter k given in the IGA software is related to D by the following equation:

$$D = \frac{l^2}{\pi^2 k} \tag{7}$$

Thus, from the k parameter given by the IGA software, D defined by long times approximation can be calculated.

Pressure decay sorption cell (PDSC)

The PDSC was a dual-volume-type cell made of stainless steel connected to a pressure transducer (TRAFAG, NA40.0A type) with a pressure range from 1 to 40 bar. The transducer signal was monitored in a personal computer with *ad hoc* software. A polymer sample of approximately 2 cm^3 was used. More details about the design and operation procedures were described elsewhere.[4,16]

Analytic gas permeability fractometer

The Lyssy (Zollikon, Switzerland) permeability apparatus (GPM 500) was an isostatic analytic gas permeability tester, which allowed the simultaneous determination of permeability to different permanent gases of a mixture. It was equipped with a GC320 gas chromatograph from GL Sciences, Inc., (Tokyo, Japan) with a thermal conductivity detector. The column was an All Tech CTR I (Deerfield, IL) column (6 × 1.4 in.) of stainless steel, and the oven temperature and pressure of the gas carrier (helium) were 50°C and 2 bar, respectively. The procedure used was as follows: once the sample was placed and the permeability chamber was sealed, the downstream chamber was purged with helium for 1 min and homogenized for another 1 min. This operation was repeated until no traces of penetrant gases were observed in the downstream side. After that, the desired flow of upstream gas was introduced, and the permeated gas was analyzed every 2 h. To obtain the permeability, a previous calibrate was necessary to correlate the chromatogram peak areas to the permeated gas amounts. In this sense, the apparatus allowed us to extract a known amount of the upstream gas and to inject it into the chromatograph. Thus, P was related to the peak areas by

$$P \propto \frac{A}{A_c/V_c} \tag{8}$$

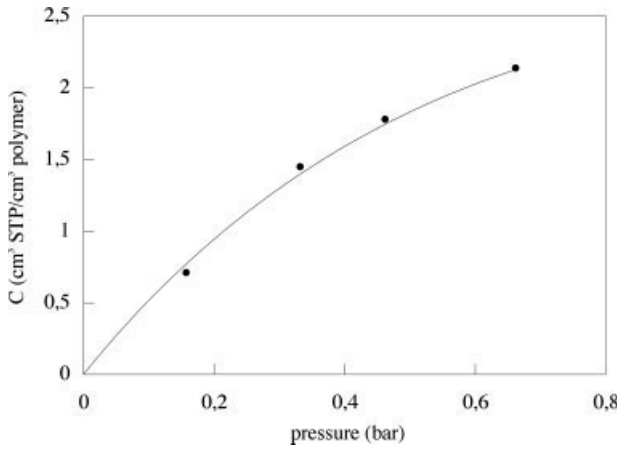

Figure 1 CO_2 isotherm in Trogamid at 30°C obtained in the Cahn balance. The solid curve is the dual-mode fit.

where A and A_c are the chromatogram peak areas of the sample measurement and of calibration, respectively, and V_c is the injected calibration sample volume. To obtain P, the proportionality constant is shown in the following equation:

$$P\left(\frac{\text{cm}^3\text{STP cm}}{\text{m}^2\text{atm day}}\right) = \frac{A}{A_c/V_c}\frac{1}{s}\frac{1}{tn/24}\frac{273}{273+T} \times l\left(1+\frac{0.8}{29.2}(n-1)\right) \quad (9)$$

where s is the film area (m^2), n is the injection number, t is the time between consecutive injections (h), T is the temperature (°C), l is the film thickness, and the term between brackets is a correction factor that takes into account the permeated gas amount extracted in the preceding injections.

RESULTS AND DISCUSSION

Solubility

The subatmospheric measurements were carried out with the Cahn electrobalance. At low pressures, the solubility usually follows Henry's law:

$$C = K_D p \quad (10)$$

where C is the concentration of dissolved gas into the polymer, K_D is Henry's law constant, and p is the pressure. Thus, C is proportional to pressure, a fact that was not fulfilled in the Trogamid/CO_2 case because in the isotherm obtained for a film of 69 μm, which is shown in Figure 1, a slight curvature for pressures above 0.5 bar was observed. This behavior is usual in polymers that are in glassy state, as occurred for Trogamid, whose glass-transition temperature was near 160°C. In such cases, a combination of the Henry and Langmuir isotherm types, known as dual model, is applied:[4,17–23]

$$C = K'_D\, p + \frac{C'_H b' p}{1 + b' p} \quad (11)$$

where C'_H and b' are the Langmuir capacity constant and the Langmuir affinity constant, respectively. K'_D measures Henry's sorption mode contribution to total sorption, but evidently its value differs from K_D obtained from eq. (10). Unfortunately, the number of subatmospheric data was not enough to adequately fit the three dual-model parameters. Actually, the C'_H, b', and K'_D parameters took values without physical meaning; for instance, K'_D had a negative value, although the fitting appearance was satisfactory, as shown in Figure 1. Because of this, we decided to calculate K_D given by eq. (10), taking into account only the sorption data corresponding to pressures below 0.5 bar and obtaining a value of 4.46 cm^3 STP cm^{-3} bar^{-1}). However, data with higher pressures confirmed the adequacy of the dual model for the Trogamid/CO_2 case.

In Figure 2, the sorption isotherm obtained with the PDSC for a similar film is compared to previous data. First, the good agreement between them can be taken as a proof of their reliability. Second, the isotherm clearly showed a curvature at high pressures, as the Cahn data suggested, so the dual model was more appropriate to fit the isotherm and to obtain sorption characteristic parameters. Now, the higher data number allowed us to fit the dual-model parameters and gave the following values: $K'_D = 0.526$ cm^3 STP cm^{-3} bar^{-1}, $C'_H = 12.26$ cm^3 STP $cm-^3$, and $b' = 0.289$ bar^{-1}. The slope of this curve at origin was compared to the Henry constant calculated by eq. (10). This slope corresponded to

$$K_D = K'_D + C'_H b' \quad (12)$$

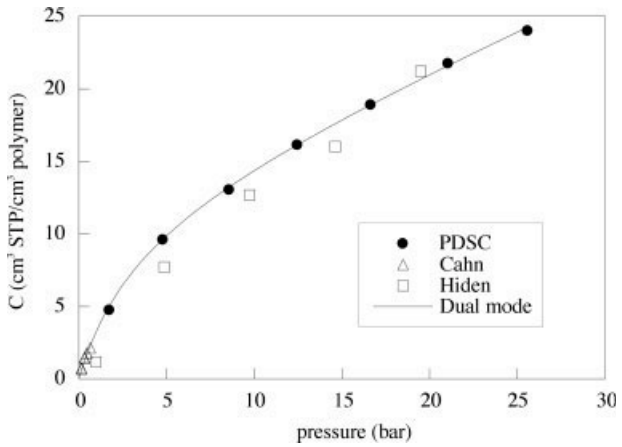

Figure 2 CO_2 isotherm in Trogamid at 30°C obtained with different equipment.

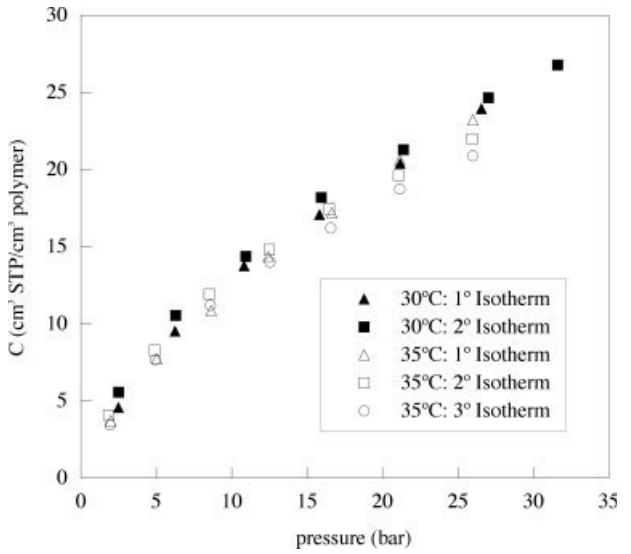

Figure 3 CO_2 subsequent isotherms in Trogamid measured in the PDSC at 30 and 35°C.

which gave a value of $K_D = 4.07$ cm^3 STP cm^{-3} bar^{-1}, which agreed with the calculated with Cahn data corresponding only to pressures up to 0.5 bar.

Moreover, the Hiden IGA electrobalance allowed us to obtain the complete isotherm in a single measurement. The measured CO_2 concentration in Trogamid is also shown in Figure 2. From this figure, we concluded that both the pressure decay and gravimetric methods were in good agreement, and in conclusion, the three tested methods gave reproducible equilibrium solubility data.

Conditioning phenomena have been reported in the literature for CO_2 gas.[24–26] In such a type of processes, after a sorption isotherm has been performed and the gas has been subsequently desorbed, the polymeric film does not return to its original state, and in a further isotherm, the film behaves as it would be plasticized. This behavior has been imputed to an increase in the free volume by inelastic changes in the polymer morphology. In this sense, two new consecutive isotherms for a film of 100 μm were determined at 30°C in the PDSC equipment, whose results are plotted in Figure 3, and we concluded that conditioning did not occur at this temperature. However, at 35°C, two subsequent CO_2 isotherms slightly deviated from the first one, as shown in Figure 3.

This conditioning effect became more evident when the dual-model parameters were calculated, as shown in Table I. K'_D defined by the dual model took smaller values in the second and third isotherms, whereas C'_H increased. This behavior could be interpreted as a probe of conditioning because it implied an increase in the Langmuir sorption, which is governed by the accommodation of particles of solute in inelastic holes, and a decrease of Henry's sorption. Plasticization implies a change in the solubility process, which is seen as an increase in C'_H.[27] Actually, in the Trogamid/CO_2 case, the increase in free volume due to the conditioning was not enough to balance the decrease that K'_D suffered as occurred in other cases.[24,25] This fact is shown in Table I, where C'_H increased slightly in the isotherms at 35°C. In conclusion, a slight conditioning of CO_2 in Trogamid appeared at 35°C. When we considered that the conditioning appeared over such a narrow temperature range, which was far below Trogamid T_g, we did not find any reason to explain this fact.

The Hiden electrobalance also allowed us to confirm the conditioning behavior. In this sense, in Figure 4, two subsequent isotherms carried out at 35°C and the first one obtained by PDSC are compared. First, at this temperature, the agreement between both types of equipment was excellent, which corroborated their reproducibility. Second, in this case, the conditioning was not observed. A possible reason for this might be the different vacuum procedures used in the desorption step. In the PDSC technique, vacuum was applied as soon as the desorption started, whereas the Hiden equipment limited the vacuum rate to 200 mbar/min. Thus, this slow desorption rate allowed the polymer to lose all the plasticized state, whereas in the PDSC case, the polymer could immediately freeze the changes promoted by the conditioning.

On the other hand, Figure 3 also shows that solubility practically did not change in the studied temperature range because both the first isotherms at 30 and 35°C were very similar.

TABLE I
Dual Model Parameters at 35°C Calculated from Subsequent Isotherms

Isotherm	T (°C)	K'_D(cm^3 STP cm^{-3} bar^{-1})	C'_H (cm^3 STP/cm^3)	b' (bar^{-1})
1	30	0.480 ± 0.05	14.17 ± 2	0.133 ± 0.03
2	30	0.458 ± 0.05	14.74 ± 2	0.169 ± 0.02
3	35	0.555 ± 0.05	11.33 ± 2	0.148 ± 0.03
4	35	0.331 ± 0.03	17.39 ± 1	0.130 ± 0.01
5	35	0.277 ± 0.04	18.97 ± 2	0.099 ± 0.01

In every case, the data obtained by the Cahn balance were considered in the fitting.

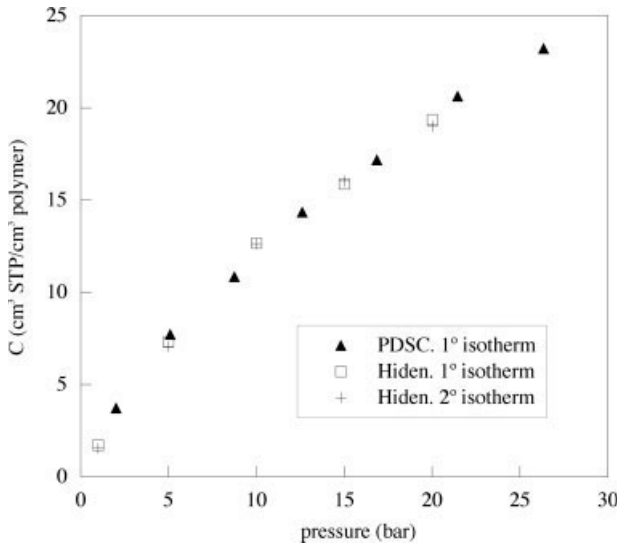

Figure 4 CO_2 subsequent isotherms in Trogamid measured in the Hiden electrobalance at 35°C.

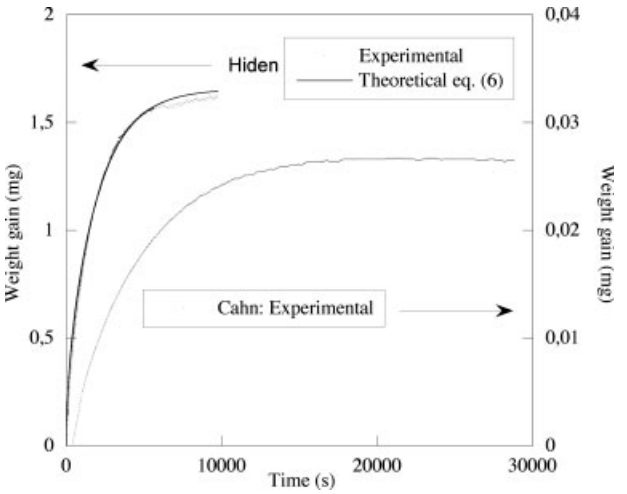

Figure 5 Kinetics obtained in the two electrobalances at 30°C: Cahn = 0.35 bar and Hiden = 5 bar.

Diffusion

As explained previously, D could be extracted from an adequate mathematical treatment of the kinetic sorption data.

Unfortunately, the pressure decay method did not allow those calculations because of the difficulty in determining both the initial pressure and time in the kinetics; thus, D values were only been calculated from the Cahn and Hiden electrobalances. In the case of the Cahn electrobalance, the long times approximation was assumed, whereas in the Hiden case, as mentioned previously, its own software allowed us to fit the kinetic data by means of a parameter that was directly related to D calculated with the aforementioned long times approximation [eq. (7)]. In this point, it must be remembered that the Hiden software truncated the kinetic when a previously fixed percentage of the final M_∞ was reached. In our case, we used the 99% value. This different procedure gave kinetics that differed in some grade from the ones obtained by the Cahn electrobalance. As shown in Figure 5, the latter kinetics took the usual shape, whereas the former ones did not yet achieve the final plateau. This truncated kinetic type would influence in the values of the determined D, but the fitting of the experimental data by eq. (6) was reasonably good. Furthermore, Balik[28] proposed the fitting of kinetic data with a method that combines both the short and long times approximations;[15] thus, we applied this so-called hybrid method to the Hiden data, and similar D values were obtained. Thus, we concluded that the Hiden procedure was appropriate to calculate reliable D values.

Focusing on D values, the results obtained from both data series are shown in Figure 6. The D values calculated from the Cahn kinetics appeared to increase with pressure, but when one considers that the D determined from the Hiden data did not depend on pressure, in our opinion, D could be taken as constant in the studied pressure range. Moreover, the average D (approximately 8×10^{-10} cm^2/s) reflected the good performance of Trogamid as barrier material to CO_2 and, thus, an adequate polymer for packaging and beverage applications.

Permeability

P could be estimated from S and D values. For instance, if Henry's law was obeyed and the equilibrium was reached, P was given by eq. (1). This simple equation shows that permeation is related to the ability to solve the penetrant and its further mobility through the membrane. Furthermore, eq. (1) allows one to deter-

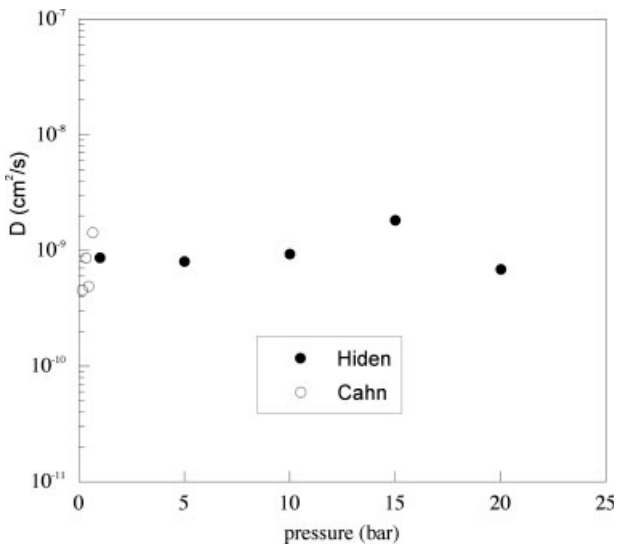

Figure 6 D of CO_2 in Trogamid at 30°C.

mine one coefficient if the other two are known. Although, as shown previously, the solubility did not strictly follow Henry's law, the *P*s were estimated by eq. (1), with solubility and *D* values determined from gravimetric measurements, and the results are plotted in Figure 7. The *P* value estimated by the Cahn balance could be considered independent of pressure as well as the data obtained from the Hiden, and although both techniques provided different *P* values, they were in a reasonable agreement. Thus, permeability was considered practically constant with pressure. Another interesting result is, as could be expected from the low values of *D* and *S*, the low values of *P*, reflecting the good barrier properties of Trogamid polyamide to CO_2.

Alternatively, the Lyssy permeability cell directly gave *P*. At 30°C and with a film of 60 μm, the measured *P* at 1 bar was 0.205 bar (see Table II), which was inside the range delimited by the values estimated by the Cahn and Hiden equipment, as shown in Figure 7. In conclusion, the estimated *P* value by eq. (1) agreed very well with the *P* value measured directly by the Lyssy equipment.

One of the advantages of the Lyssy permeability cell was the fact that the gas chromatograph used to measure the amount of permeated gas allowed us to obtain simultaneously the *P*s of different gases when a gas mixture was flowed upside the membrane; thus, this technique directly provided the real permselectivity $\alpha_{A/B}$ defined by

$$\alpha_{A/B} = \frac{P_A}{P_B} \tag{13}$$

where P_i is the permeability coefficient of penetrant *i*. The permselectivity reflects the ability of a material to separate two gases that are mixed in the upstream side, and it is a very interesting to characterize the transport properties of any material. Moreover, the experimental techniques that provide the real permselectivity are scarce, and instead of the real permselectivity value, commonly, an ideal one is used.[29] The ideal permselectivity is given by the same eq. (13) but with the P_i of pure gases. In this sense, the Lyssy permeability cell allowed us to compare the real and ideal permselectivity values. In Table II, the *P*s for pure CO_2, O_2, and N_2 and for an equimolecular mixture of the former gases are shown.

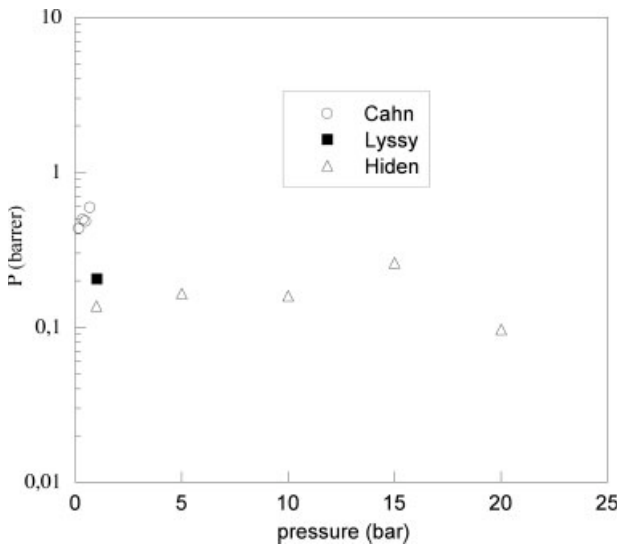

Figure 7 *P* of CO_2 through Trogamid at 30°C.

TABLE II
Permeability of Atmospheric Gases Through Trogamid at 1 bar and 30°C

	P (Barrer)	
	Pure gas	Gas mixture
CO_2	0.205 ± 0.008	0.235 ± 0.015
O_2	0.058 ± 0.003	0.079 ± 0.009
N_2	0.024 ± 0.002	0.048 ± 0.010

From the comparison of data, both CO_2 and O_2 *P*s increased slightly when they were mixed, so the presence of other gases expedited their permeation rate. However, in the case of N_2 gas, its *P* increased strongly (ca. 100% from pure gas to mixture). Because Trogamid had a glassy nature, at 30°C, two facts could occur in relation to solubility. If gas molecules compete for specific sorption sites, the individual solubility decreases. However, if a plasticization phenomenon happens, as usually occurs with CO_2, the low solubility component suffers a huge increase.[30,31] Moreover, the presence of other gases also affect the diffusion process. In this case, CO_2 and, possibly at a lower level, O_2, was responsible for the larger diffusion rate of N_2 due to a diffusion path opening effect. Again, the two aforementioned facts play an important role, and a decrease in permselectivity would be expected when plasticization becomes more significant.[30]

A dual-mode partial immobilization model for glassy polymers[32] was developed for glassy polymers and a modified dual model to take into account plasticization behavior[33] where diffusivity would increase with sorbed gas concentration. Unfortunately, we could not dispose of more data at higher pressures to study in depth the real permselectivity of Trogamid. In conclusion, because the real permselectivity of the O_2/N_2 pair, and for CO_2/N_2 and CO_2/O_2, decreased substantially from the ideal one, we concluded that plasticization played a more major role than the competence between the different gases for specific sorption sites.

Anyway, the real permselectivity differed substantially from the ideal one. For instance, for the O_2/N_2 pair, the ideal permselectivity was 2.4, whereas the real one took a value of 1.65. This difference gave us an idea about the error that one can make with ideal permselectivity instead of the real one.

TABLE III
Permeability of an Atmospheric Gas Mixture Through Trogamid at 1 bar and 35°C

	P (Barrer)
CO_2	0.229 ± 0.004
O_2	0.103 ± 0.004
N_2	0.151 ± 0.007

Furthermore, we studied the change of the permselectivity with temperature. The *P* values of the three gases in the mixture are compiled in Table III. When these data are compared to those in Table II, the N_2 behavior must be emphasized. Although CO_2 *P* remains constant and O_2 *P* had a slight increase, N_2 *P* was three times bigger than at 30°C. In general, temperature improved the diffusion processes for all of the gases, but the solubility variation was different for no condensable gases, such as O_2 and N_2, and for more interacting gases, such as CO_2. Although in the former case, solubility increased with temperature, in the latter one, it decreased, even though there we did not observe differences in the solubility of CO_2 between both temperatures (see Fig. 3). In the case of Trogamid, both effects balanced for CO_2, but for N_2 and O_2, those effects added one to each other. The large increase in the permeability of the smallest molecule (N_2) reflected that the diffusion must have had a stronger effect on the permeability. Thus, the real permselectivity of the O_2/N_2 pair changed substantially. At 35°C, $\alpha_{A/B}$ fell from 1.65 (30°C) to 0.68; thus, the permeated gas mixture got richer in N_2, whereas at 30°C, it was richer in O_2. This result shows us the important role of temperature in the permselectivity and, therefore, in the optimal conditions for a gas-separation process.

CONCLUSIONS

Three different sorption experimental techniques were compared, two of them having a gravimetric basis. Although the Hiden electrobalance allowed us to achieve pressures from a subatmospheric range up to 20 bar, the Cahn electrobalance only covered the subatmospheric range. The third technique had a barometric basis and covered pressures from 1 to 30 bar. The *S* values obtained by those techniques were in good agreement for CO_2 in Trogamid at 30°C, which showed the reliability of the techniques. On the other hand, the solubility followed the dual-sorption mode, even at subatmospheric pressures. Furthermore, a slight conditioning behavior appeared for the first time at 35°C, a fact that was reflected in the decrease of Henry's sorption mode contribution opposite the increase observed for the Langmuir term contribution to the total solubility.

In relation to the diffusion process, both electrobalances, even with the truncated shape of the kinetics obtained in the Hiden one, gave comparable *D* values for CO_2 in Trogamid. Furthermore, a more complete data treatment gave *D* values in a good agreement; thus, the Hiden software was able to calculate reliable values of both *S* and *D*. The absolute value of *D* took a relatively small value (ca. 8×10^{-10} cm^2/s) independent of pressure.

*P*s estimated from *S* and *D* values by both electrobalances were also in good agreement with the obtained one directly in a permeation cell (Lyssy). Furthermore, *P*s of Trogamid/CO_2 pair had small values, which reflected its good barrier properties. Also, the results obtained from the Lyssy apparatus pointed out another interesting fact: the real permselectivity could deviate substantially from the ideal one, as occurred for the O_2/N_2 pair in Trogamid, where the real value was half of the ideal one. This behavior could arise from a diffusion path opening effect because bigger molecules (CO_2 and O_2 in our case) provide the permeation process to smaller ones (N_2). Moreover, a small temperature increase drove the inversion on the permselectivity value: at 30°C, the permeated gas got richer in O_2, whereas at 35°C, it got richer in N_2.

References

1. Felder, R. M.; Huvard, G. S. Methods of Experimental Physics; Polymers Part C 16; Academic: New York, 1980; Chapter 17.
2. Crank, J.; Park, G. S. Diffusion in Polymers; Academic: London, 1968.
3. Koros, W. J.; Paul, D. R.; Rocha, A. J Polym Sci Polym Phys Ed 1976, 14, 687.
4. Koros, W. J.; Paul, D. R. J Polym Sci Polym Phys Ed 1976, 14, 1903.
5. Weinkauf, D. H.; Kim; D. H.; Paul, D. R. Macromolecules 1992, 25, 788.
6. Ghosal, K.; Freeman, B. D.; Chern, R. T.; Alvarez, J. C.; de la Campa, J. G.; Lozano, A. E.; de Abajo, J. Polymer 1995, 36, 793.
7. McHattie, J. S.; Koros, W. J.; Paul, D. R. Polymer 1992, 33, 1701.
8. Wang, Z.; Chen, T.; Xu, J. Macromolecules 2001, 34, 9015.
9. Koros, W. J. Barrier Polymers and Structures; Koros, W. J., Ed.; ACS Symposium Series 423; American Chemical Society: Washington, DC, 1990; Chapter 1.
10. Lagaron, J. M.; Gimenez, E.; Gavara, R.; Saura, J. J. Polymer 2001, 42, 9531.
11. De Petris, S.; Laurienzo, P.; Malinconico, M.; Pracella, M.; Zendron, M. J Appl Polym Sci 1998, 68, 637.
12. Matayabas, J. C., Jr.; Turner, S. R. Polymer–Clay Nanocomposites; Pinnavaia, T. J.; Beall, G. W., Eds.; Wiley: Chichester, England, 2000; Chapter 11.
13. Yamamoto, K.; Maruo, K.; Okada, S.; Maruyama, K. (to Mitsubishi Gas Chemical Co., Ltd.). Jpn. Pat. 2001354222 (2001).
14. Akkapeddi, M. K.; Socci, E. P.; Kraft, T. J.; Worley, D. C.; Pratt, J. D.; Brown, C. V. (to Honeywell International, Inc.). U.S. Pat. 6,410,156 (2002).
15. Crank, J. S. Mathematics of Diffusion; Clarendon: Oxford, 1975.
16. Barbari, T. A. Ph.D. Thesis, University of Texas, 1986.
17. Masi, P.; Paul, D. R.; Barlow, J. W. J Polym Sci Part B: Polym Phys 1982, 20, 15.
18. Toi, K.; Morel, G.; Paul, D. R. J Appl Polym Sci 1982, 27, 2997.

19. Barbari, T. A.; Koros, W. J.; Paul, D. R. J Polym Sci Part B: Polym Phys 1988, 26, 709.
20. McHattie, J. S.; Koros, W. J.; Paul, D. R. Polymer 1991, 32, 840.
21. Toi, K.; Ito, T.; Shirakawa, T.; Ikemoto, I. J Polym Sci Part B: Polym Phys 1992, 30, 549.
22. Reimers, M. J.; Barbari, T. A. J Polym Sci Part B: Polym Phys 1994, 32, 131.
23. Barbari, T. A. J Polym Sci Part B: Polym Phys 1997, 35, 1737.
24. Jordan, S. M.; Koros, W. J.; Fleming, G. K. J Membr Sci 1987, 30, 191.
25. Wang, J.-S.; Kamiya, Y.; Naito, Y. J Polym Sci Part B: Polym Phys 1998, 36, 1695.
26. Coleman, M. R.; Koros, W. L. Macromolecules 1999, 32, 3106.
27. Fleming, G. K.; Koros, W. J. Macromolecules 1986, 19, 2285.
28. Balik, C. M. Macromolecules 1996, 29, 3025.
29. Ruiz-Treviño, F. A.; Paul, D. R. J Appl Polym Sci 1998, 68, 403.
30. Paul, D. R.; Yampol'skii, Y. P. Polymeric Gas Separation Membranes; CRC: Boca Raton, FL, 1994.
31. Bitter, J. G. A. Transport Mechanisms in Membrane Separation Processes; Plenum: New York, 1991.
32. Koros, W. J.; Chern, R. T.; Stannet, V. T.; Hopfenberg, H. B. J Polym Sci Part B: Polym Phys 1981, 19, 1513.
33. Zhou, S.; Stern, S. A. J Polym Sci Part B: Polym Phys 1989, 27, 205.